Natural Resources Canada | Ressources naturelles Canada

GEOLOGICAL SURVEY OF CANADA
OPEN FILE 8725

A compilation of microtremor horizontal-to-vertical spectral ratios (HVSRs) and borehole shear-wave velocities of unconsolidated sediments in south-central Ontario

J.A. Hunter, H.L. Crow, B. Dietiker, A.J.-M. Pugin, K. Brewer, and T. Cartwright

2020

Canada

GEOLOGICAL SURVEY OF CANADA
OPEN FILE 8725

A compilation of microtremor horizontal-to-vertical spectral ratios (HVSRs) and borehole shear-wave velocities of unconsolidated sediments in south-central Ontario

J.A. Hunter, H.L. Crow, B. Dietiker, A.J.-M. Pugin, K. Brewer, and T. Cartwright

Geological Survey Canada, 601 Booth Street, Ottawa, Ontario K1A 0E8

2020

Permanent link: https://doi.org/10.4095/326133

This publication is available for free download through GEOSCAN (https://geoscan.nrcan.gc.ca/).

Recommended citation
Hunter, J.A., Crow, H.L., Dietiker, B., Pugin, A.J.-M., Brewer, K., and Cartwright, T., 2020. A compilation of microtremor horizontal-to-vertical spectral ratios (HVSRs) and borehole shear-wave velocities of unconsolidated sediments in south-central Ontario; Geological Survey of Canada, Open File 8725, 1 .zip file. https://doi.org/10.4095/326133

Publications in this series have not been edited; they are released as submitted by the author.

1. INTRODUCTION

Horizontal-to-vertical spectral ratios (HVSRs) of microtremor-generated ambient noise were obtained during the 2015-2017 field seasons at 41 borehole sites in south-central Ontario, where in-hole measurements of shear-wave velocity-depth structure had previously been made. It has been shown that HVSR spectral resonance maxima are directly correlated either to the presence of large seismic impedance contrasts within the unconsolidated sediments above the bedrock contact, or to the sediment-bedrock boundary (Molnar et al., 2018). Ongoing research is currently examining the peak amplitudes and shapes of the HVSR resonance maxima in order to correlate with known subsurface structure of unconsolidated sediments in Canada. This present work is a contribution towards such correlations with respect to variable shear-wave velocity structure, as shown through comparison of down-hole velocity logs with co-located microtremor HVSRs.

In recent years, the use of HVSR techniques has been increasingly applied in various areas worldwide to aid in the investigation of soft soil earthquake amplification and near-surface structural studies in zones where unconsolidated sediments overlie firm bedrock (Molnar et al., 2018). In Canada, work has been successfully carried out by the Geological Survey of Canada (GSC) and others in several soft soil areas in British Columbia (Fraser River Delta, Kitimat Valley) and in several areas of Eastern Canada (Niagara peninsula, the Ottawa Valley region of Eastern Ontario, the Montreal area (Rosset and Chouinard, 2009), Lac St. Pierre region, Baie St. Paul region, and Quebec City, as well as the city of Fredericton). In most of the areas studied, post-glacial sediments overlie either firm Pleistocene sediments or bedrock directly, and the seismic impedance contrasts at the boundaries are large (as shown from borehole geophysical measurements of density and shear-wave velocity; Pullan et al., 2002; Crow et al., 2015). As well, because of the large seismic contrasts at the base of soft soils, large amplifications of small strain earthquakes have also been observed at ground surface at some locations (e.g. Crow et al., 2011; Motazedian et al., 2011; Motazedian et al., 2020).

Commonly, it has been assumed that Pleistocene glacial sediments overlying firm bedrock yield relatively small impedance contrasts which would result in lower or uninterpretable resonant HVSR maxima. Correspondingly, there would be much less earthquake site amplification attributed to the seismic impedance boundary. However, recent HVSR tests, in association with GSC high-resolution near-surface seismic reflection surveys in these terrain types, have indicated significant interpretable spectral resonance peaks occurring at many sites, causing us to revise our previously held opinions. This has led us to develop a routine comparison of HVSR spectra at geotechnical field sites in glacial deposits of south-central Ontario, where down-hole shear-wave velocity-depth determinations are available, as reported herein.

2. SITE LOCATIONS

During the 2015-17 field programs, HVSRs were obtained at previously drilled borehole sites as shown in Figure 1.

All boreholes were PVC-cased and logged with down-hole geophysical techniques in previous years by the Ontario Geological Survey, the Geological Survey of Canada, and with the co-operation of several Ontario Government Regional Groundwater Mapping programs. The complete suite of geophysical logs, along with the detailed geology obtained from core recovery, location and well ownership, are given by Crow et al. (2015). Borehole identifications, UTM locations, borehole depths and depth to bedrock are given in Table 1 of this report.

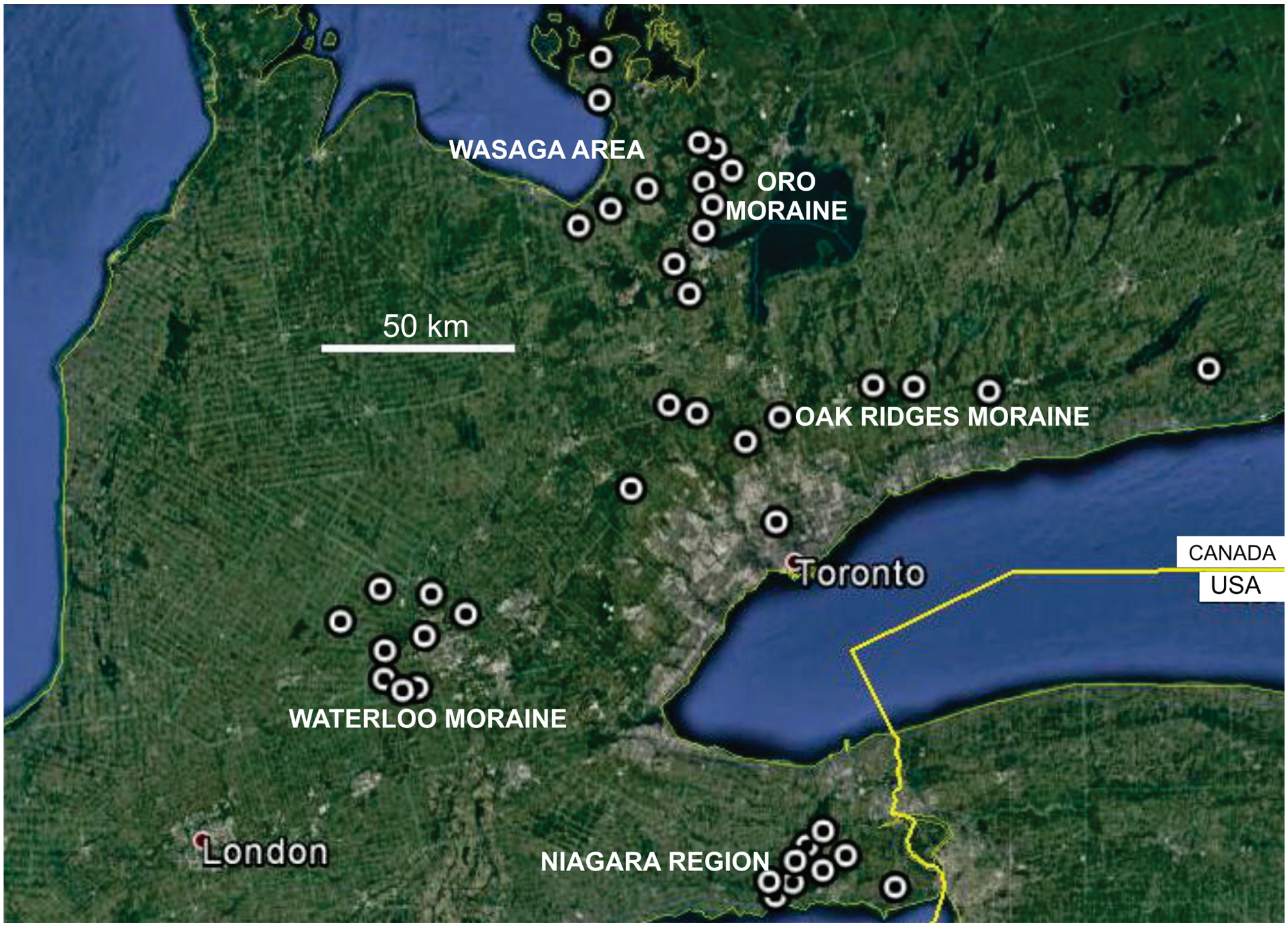

Figure 1. Location of geophysical boreholes in south-central Ontario (© Google Earth, 2019).

3. BOREHOLE SHEAR-WAVE MEASUREMENT TECHNIQUES

The down-hole shear-wave seismic surveys were carried out in the cased boreholes using a 3-component casing-clamped down-hole sonde with 15 Hz geophones and an energy source on the surface near the borehole collar. The cable supporting the sonde was lowered by hand to the bottom of the hole, and raised up-hole at 0.5 or 1 m intervals. At each depth, background ambient noise was allowed to stabilize after clamping before stationary surface-to-sonde shear-wave travel-time measurements were recorded. The source was a metal sledge-hammer, striking a metal plate at a 45° angle from the ground surface (to generate S-wave energy) at 1-m, 3-m or 5-m offsets from the borehole. The plate was coupled with the ground by removing the top few centimeters of soil, leveling the plate, and then driving the wheel of a heavy vehicle onto it to seat it in place. A Geometrics Geode seismograph was used and data were recorded on a laptop computer after reviewing each record on screen. The systems and field procedures developed for down-hole P- and S-wave logging are described in detail in Hunter et al. (1998) and Pullan et al. (2002).

4. SURFACE HVSR MEASUREMENT TECHNIQUES

Data were obtained using Tromino Seismographs (Model TEP made by MOHO Science and Technology Co). These units each contain 3 orthogonal broadband velocity sensors (± 1.2 mm/s range) and 3 orthogonal accelerometers (± 2g). At most borehole sites, two independent units were installed in firm ground within a few meters of each other and recorded for similar time periods (30 minutes).

Individual spectra were computed for each 30-second time period, yielding a maximum of 60 separate spectra per site per unit. During the processing, individual H/V spectra showing local noise contamination, were removed from the dataset. The purged Horizontal/Vertical frequency component data were then processed, utilizing proprietary GRILLA software sold by MOHO and following recommended procedural guidelines given by the SESAME European consortium (SESAME 2004).

5. COMPILATION OF RESULTS

APPENDIX A: Down-hole Shear-Wave Digital Data

The EXCEL files in this appendix contain compilations of the down-hole shear-wave travel-times, average shear-wave velocities (Vsav), and interval shear-wave velocities (Vsint) with depth for each borehole site. The seismic data were extracted and edited from the above-mentioned Open File 7591 by Crow et al. (2015).

APPENDIX B: Combined Plots of HVSR, Borehole travel-times, Vs, and Generalized Geology

For each site, in the order given in Table 1, plots of both down-hole average Vs (Vsav) and interval Vs (Vsint) values versus depth below surface are compared to interpreted frequency spectra of HVSR data. The upper part of each figure shows a plot of depth vs down-hole shear-wave travel-time, Vsav, and Vsint, as well as a general description of the material type (and formation name where identified). The lower part of each diagram shows the H/V processed spectral ratio along with the estimated resonant peak frequency; note that the statistical error given is 2× standard error, or 95% confidence limits.

Note: The boreholes examined in this report commonly did not penetrate into the bedrock sufficiently to obtain reliable estimates of rock velocities. For modelers, who may require bedrock shear-wave velocity information, estimated rock Vsint values can be assigned based on compiled rock velocity analyses of similar lower Paleozoic and Precambrian rocks given by Hunter et al. (2010) for the Ottawa region. Such velocities may range between 1900 and 3500 m/s.

APPENDIX C: Recorded Microtremor Time Series

The raw ambient 3-component noise ground velocity, in 30-minute time series, are given in mm/s and in both .TXT and .SAF formats. The data have been corrected (calibrated in mm/s ground velocity) for instrument response between 0.3 Hz and 50 Hz. Metadata describing each measurement can be found in Table C-1 in Appendix C.

Table 1: Borehole locations, depth and interpreted HVSR resonances

Borehole Name	UTM East (m) Zone 17T	UTM North (m) Zone 17T	Depth of BH (m bgs)	Depth to Rock (m bgs)	HVSR Site Name	Resonance Frequency Fo (Hz)	Error in Fo $\pm 2\sigma$	Period To (s)	Depth to Resonator (To*Vsav/4) (m)
OAK RIDGES MORAINE									
Aurora	626137	4871862	140.8	138.5	AUR-1	1.44	0.01	0.694	104
Caledon East	588632	4852726	180	179.2	Caledon-2	0.84	0.03	1.190	121
GLL-1 Coppins	649822	4880649	124	N/A	GRASS-2	1.19	0.02	0.840	118.5
GLL-2 Grasshopper	679521	4879974	140	136.7	GLL-2	4.72	0.28	0.212	34
GLL-2 Grasshopper	"	"	"	"	"	2.0	0.33	0.500	100 est
King City	617528	4865460	190	N/A	KINGCITY-1	0.94	0.07	1.064	127.5
North York EBA	625954	4845255	90	86	Earl Bales BH EB	1.33	0.03	0.752	90?
Port Perry-Utica	660237	4880592	125.3	122.5	PORTPERRY-2	12.75	0.39	0.078	19.6
RiceLake-Centreton	736001	4887350	180	176.7	RICE-1	1	0.03	1.000	169?
Schomberg	604983	4872326	140.3	N/A	SCHOM-2	0.91	0.005	1.099	151
NIAGARA									
Niagara 05	632560	4753345	48.4	45.15	WELL-8 NIAG BH5	1.66	0.05	0.602	31
Niagara 08	626541	4753495	47.35	44.5	WELL-7 NIAG BH8	2.22	0.016	0.450	28
Niagara 09	640009	4766739	68.07	64.75	Well-18	1.56	0.01	0.641	58
Niagara 10	635967	4762870	58	55	WELL-2	1.38	0.005	0.725	43.5
Niagara 13	628215	4749786	45.72	42.7	NIAG BHOGS-13	1.44	0.02	0.694	33
Niagara 14	640187	4756676	42.06	38.7	NIAG BHOGS-14	1.78	0.02	0.562	24.5
Niagara 15	645987	4760619	43.2	40.4	NIAG BHOGS-15	1.66	0.01	0.602	36.9
Niagara 24	658861	4752849	33.48	30.1	NIAG BHOGS-24	2.13	0.03	0.469	24
Niagara 27	633076	4758904	47.95	51.05	WELL-10	1.38	0.01	0.725	36
WATEROO MORAINE AREA									
OGS03-1	547222	4819689	50	46.6	OGS03-1	3.41	0.07	0.293	33.5
OGS03-2	538290	4824574	50	47	OGS03-02R	14.97	0.07	0.067	7.3
OGS03-2	"	"	"	"	OGS03-02R	2.91	0.15	0.344	65
OG03-3	525154	4825510	90	85.5	OGS03-03R	1.53	0.06	0.654	72.4
OGS03-4	526733	4809858	95	89.1	OGS03-04	1.38	0.06	0.725	84

Borehole Name	UTM East (m) Zone 17T	UTM North (m) Zone 17T	Depth of BH (m bgs)	Depth to Rock (m bgs)	HVSR Site Name	Resonance Frequency Fo (Hz)	Error in Fo ± 2σ	Period To (s)	Depth to Resonator (To*Vsav/4) (m)
OGS03-5	515170	4816991	102	100	OGS03-05R	4.23	0.08	0.236	31.5
OGS03-5	"	"	"	"	"	2.17	0.17	0.461	78.2
OGS03-6	526685	4802636	65	62.2	OGS0-06	2.41	0.03	0.415	70 ?
OGS03-7	531491	4799815	60	58	OGS03-07	2.38	0.14	0.420	60 ?
OGS03-8	535229	4800608	80	77.6	OGS03-08	2.25	0.04	0.444	40.5
OGS03-9	536759	4813846	62	56.9	OGS03-09	2.44	0.06	0.410	52
ORO MORAINE AREA									
Barrie-Coldwell	598114	4910285	116	114.5	GSC-BH-BAW-01	1.19	0.06	0.840	82.5
Barrie-Cundles	605444	4919007	114	107	BH-02-SRS-2004	1.41	0.05	0.709	58.2
Bradford OGS BF-1	597744	4874256	148	146	BF-1	1.19	0.02	0.840	90
Bradford OGS BF-3	602214	4902750	146	N/A	BF-3	1.16	0.07	0.862	126
ORO Horseshoe Valley	605145	4931428	70	N/A	BH-06-AKB-2004	0.91	0.02	1.099	165 ?
ORO Mt St Louis	603661	4941615	105	N/A	BH-11-AKB-2004	1.13	0.04	0.885	88
ORO Mt St Louis	"	"	"	"	"	1.72	0.04	0.581	165?
ORO Dalston	607542	4925632	105	N/A	BH-13-AKB-2004	1.53	0.03	0.654	73
ORO Carley	607989	4940033	70	64.8	BH-18-AKB-2004	1.81	0.03	0.552	44
ORO Coulson	612253	4934588	56	N/A	BH-19-AKB-2004	1.38	0.03	0.725	136?
WASAGA REGION									
Wasaga CS-15-03	590587	4929374	142	135	WAS-7 BH CS-15-03	1.19	0.02	0.840	93
Wasaga CS-16-01	581428	4924041	97	93	WAS-6 BH CS-16-01	1.47	0.03	0.680	77
Wasaga CS-16-04	577807	4951821	65	62	WAS-2 BH CS 16-04	15.75	0.06	0.063	16
Wasaga CS-16-04	"	"	"	"	"	2.69	0.06	0.372	79
Wasaga CS-16-05	577815	4962960	141	N/A	WAS-3 BH CS 16-05	1.09	0.01	0.917	134
Wasaga CS-16-06	573347	4919449	85	82	WAS-8 BH CS-16-06	1.75	0.03	0.571	80

6. SOME OBSERVATIONS

The combined borehole geology, shear-wave travel-times, shear-wave average (Vsav), interval velocities (Vsint), and HVSR spectral plots are shown in Appendix B. Using the peak amplitude shown on each HVSR spectral plot, the fundamental frequency (Fo) associated with the site has been determined; note that the statistical error for Fo listed on the plot and in Table 1 is $\pm$ 2 standard error or ~ 95% confidence limit.

The fundamental site period is:

To = 1/Fo…………………………………………………. (1)

and the Equivalent-Single-Layer resonance period is given by:

To= 4H/Vsav………………………….………………….. (2)

Where:

H = depth to seismic impedance boundary

Vsav= average shear-wave velocity of a vertically incident wave traveling from the boundary to surface.

The Equivalent-Single-Layer travel-time (TT) from surface to the impedance boundary is then:

TT = To/4……………………..……………………………… (3)

By locating TT on the borehole shear-wave travel-time vs depth plots, it is possible to estimate the depth to the impedance boundary and to correlate this with possible changes in slope of the TT vs depth, Vsav vs depth and Vsint vs depth plots. These are shown on each of the plots as solid red lines with the 95% confidence limit marked as dashed red lines. From closer examination of each plot, some characteristics can be noted:

Almost all of the sites indicate at least one significant HVSR spectral peak (having an H/V ratio >2). The fundamental frequency is commonly assumed to be associated with the largest seismic impedance contrast at the overburden-bedrock boundary.

At some borehole sites (GLL-2 Grasshopper, Port Perry-Utica, OGS03-05 Wellesley, and ORO Mount St. Louis), second significant peaks at higher frequency (shallower depths) have been observed (usually <10 Hz). These are commonly associated with large Vsint contrasts within the overburden, either as velocity inversions or as high-velocity inclusion layers.

Where large Vsint variations occur within the overburden, the low-frequency resonant peak appears to be somewhat attenuated and/or broadened (e.g. Aurora, GLL-1 Coppins, GLL-2 Roseville, King City, Port Perry, OGS03-2 Elmira, OGS03-5 Wellesley, OGS03-7 Plattsville, OGS03-8 New Dundee, OGS03-9 Waterloo, BH-19-AKB-2004 Coulson, Wasaga CS-15-03, Wasaga CS-16-04, Bradford SS-12-02). However, a few other sites, with substantial high Vsint layers (~1000 m/s) at shallow depths, appear to indicate only moderate shape modifications of the low frequency Fo (Rice Lake, Schomberg, OGS03-6 New Hamburg).

At one location, BH-13-AKB-2004 Dalston, an overconsolidated till lens occurs in a lower portion of the section (73-97 m depth). There appears to be only one prominent peak, which is associated with the top of this layer, without any indication of Fo associated with the bedrock surface seismic impedance (below the bottom of the borehole at 105 m depth).

In order to assess a potential relationship between the low frequency Fo and the bedrock surface, the depth of the impedance boundaries, computed from the intersection of the down-hole shear-wave travel-times, were plotted against measured bedrock depths as determined from borehole drilling. Figure 2(a-c) shows the results from 32 borehole sites, comparing measured bedrock depth to Fo, To, and the resonator depth, as determined from the borehole shear-wave one-way travel-time. Figure 3(a-c) shows the results when comparing measured depth of the nearest impedance boundary to Fo, To, and the resonator depth, as determined from the borehole shear-wave one-way travel-time. There is a wide scattering of points in the comparisons with Fo and To, but a much better trend when the travel-time depth information is used with the HVSR peak. Note the systematic trend towards shallower depths of the HVSR estimates; this might suggest that the Fo is affected by large Vsint variations at shallower depths above bedrock, or alternatively, the HVSR at lower frequency is formed from the impedance boundary at the top of higher velocity basal unconsolidated sediments, rather than the overburden-bedrock impedance boundary beneath. There may be an additional effect of an overall velocity gradient with depth as discussed by Dobry et al. (1976), whereby a significant Vsint velocity-depth increase within a layer may result in observed higher frequency resonances than an Equivalent-Single-Layer overburden velocity model.

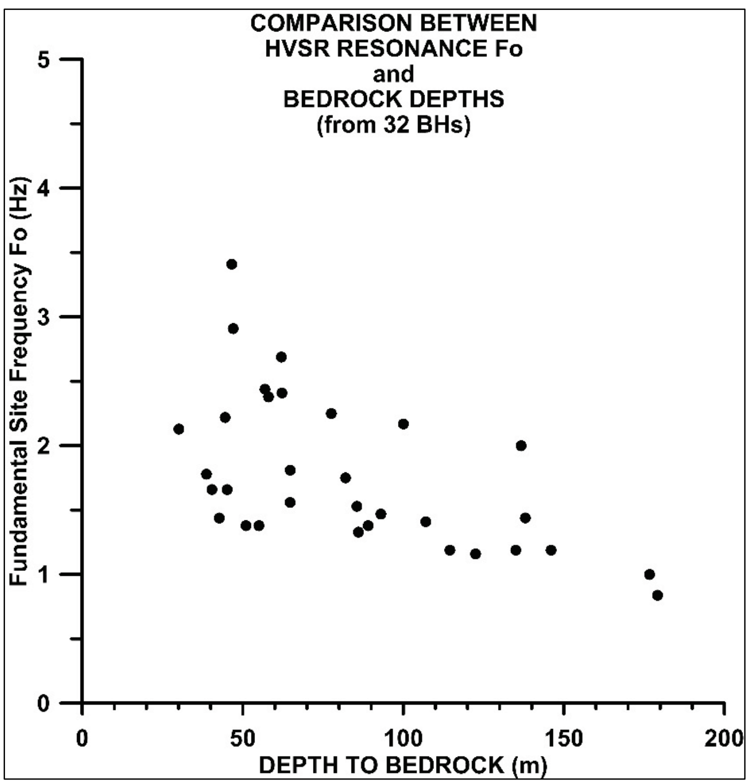

Figure 2(a)

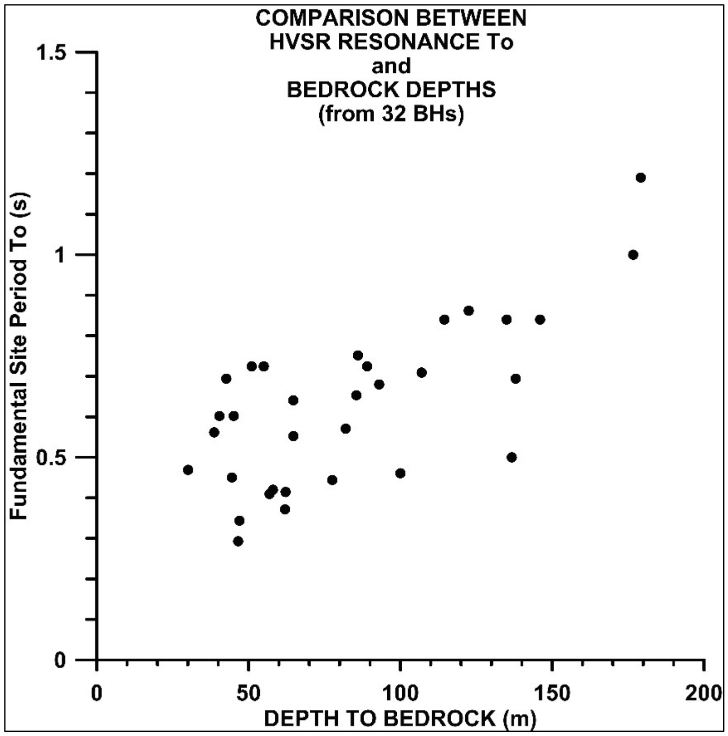

Figure 2(b)

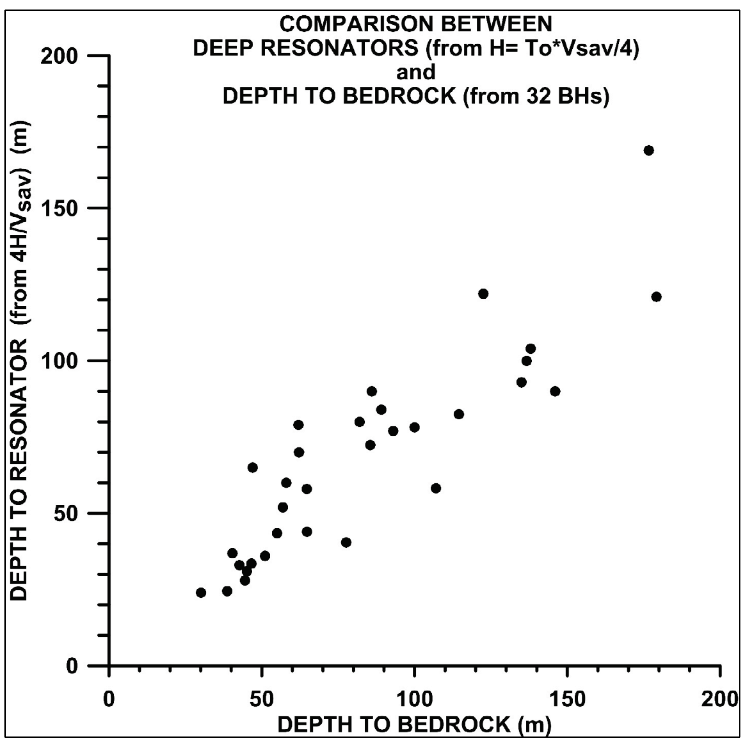

Figure 2(c)

Figure 2: Plots of depths to bedrock compared to measured HVSR Fo (a) and To (b). Using the additional down-hole travel-time and velocity information to estimate depth to resonator (c), this cluster of 32 data points shows a better linear grouping.

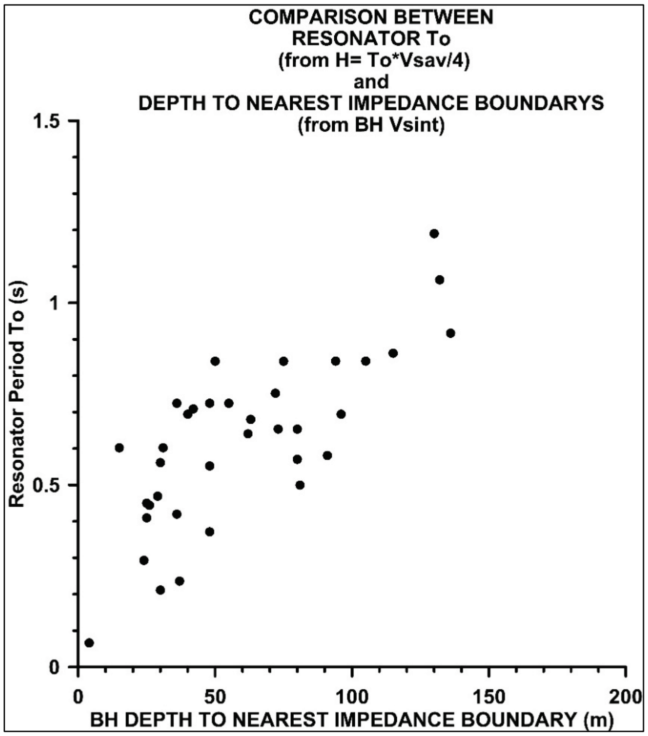

Figure 3(a)

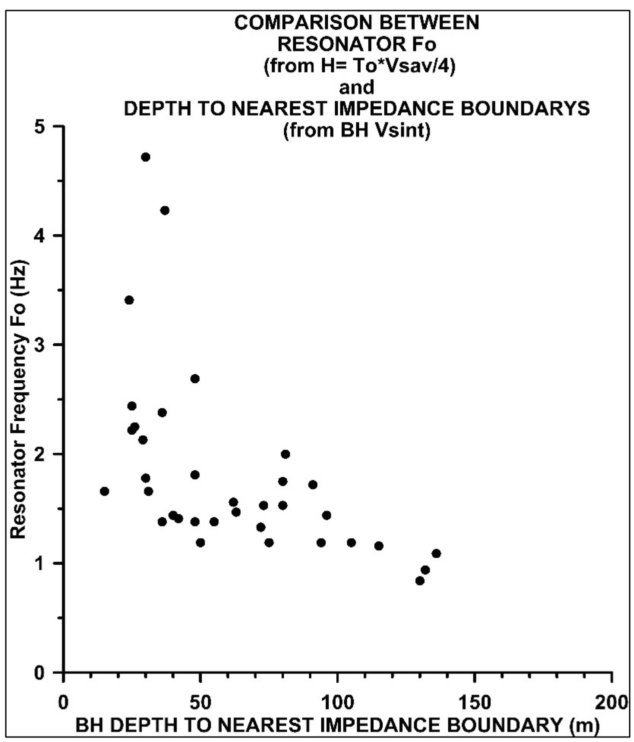

Figure 3(b)

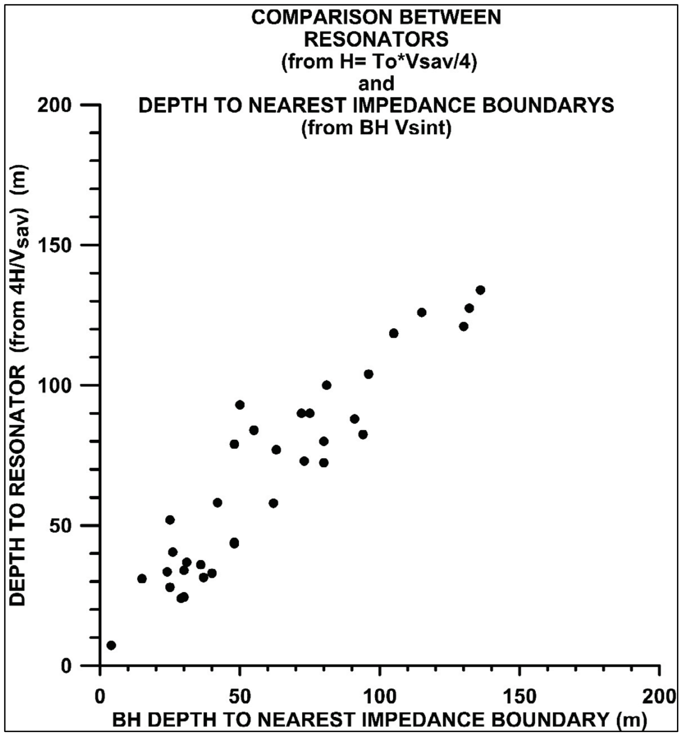

Figure 3(c)

Figure 3 shows plots of depths to nearest impedance boundaries determined from HVSRs compared to measured Fo (a) and To (b) and HVSR depth estimates, (c) compared to the depths to the nearest large impedance contrasts shown by Vsint borehole measurements (from either above or below the HVSR depth boundaries). As shown in Figure 3(c), using the additional down-hole travel-time and velocity information, this cluster of 35 data points shows a better linear grouping.

DISCUSSION

Although the database of only 41 borehole sites with down-hole shear-wave velocity and HVSR measurements is rather limited, there is enough information contained herein to suggest that shear-wave velocity-depth data and the resulting observed HVSRs are extremely variable within Pleistocene age sediments. Unlike areas of young Holocene-age surface sediments deposited under uniform conditions over widespread areas (e.g., the fine grained Champlain Sea sediments in the Ottawa and St. Lawrence River valleys), the Pleistocene-age glacial sediments at the sites examined in south-central Ontario, do not exhibit any single identifiable uniform shear-wave velocity-depth curve. Extreme variability of the measured velocity-depth data shown in this report suggests that measured HVSRs in the study area should (and do) exhibit extremely variable HVSR spectral peaks and spectral shapes. In some regions of south-central Ontario (e.g. the Niagara-Welland area), where the degree of uniformity in sediment deposition is higher, it may be possible to develop local relationships between Fo, To, and resonator depths, but only if there is sufficient ground truth in the form of sub-surface shear-wave velocity measurements to use as a base. In future, such data may be obtained by further applications of surface arrays and borehole seismic methodology.

Based on comparison of HVSRs obtained from earthquake records on soil and adjacent ambient teleseismic noise at several eastern Ontario soil sites (Motazedian et al., 2011) the two HVSR spectra sets are closely matched. Hence, these measurements are a good guide to the expected free-field resonance at any building site. It is also suggested that there may be extreme variability in ambient noise shaking spectra over short distances at sites throughout south-central Ontario, where there is Pleistocene sediment cover, and that no one set of spectral curves should be extrapolated for any significant lateral distance from a measurement site. Ground resonance is necessary for design and construction purposes, hence several on-site measurements should be performed to assure reliable spectral responses throughout the project area (Hunter and Crow, 2012).

8. ACKNOWLEDGMENTS

The authors would like to thank Abigail Burt, Riley Mulligan and Andy Bajc of the Ontario Geological Survey for early access to borehole data to allow for geophysical down-hole and surface measurements. This study was supported by the Geological Survey of Canada under the Public Safety and Groundwater Geoscience Programs.

9. REFERENCES

Crow, H.L., Hunter, J.A., Motazedian, D. 2011. Monofrequency *Insitu* damping measurements in Ottawa area soft soils; Journal of Soil Dynamics and Earthquake Engineering, v.31, p. 1669-1677.

Crow, H.L., R.L. Good, J.A. Hunter, R.A. Burns, A. Reman, H.A.J. Russell. 2015. Borehole geophysical logs in unconsolidated sediments across Canada. Geological Survey of Canada Open File No. 7591.

Dobry, R., I. Oweis, A. Urzua. 1976. Simplified procedures for estimating the fundamental period of a soil profile. Bulletin of the Seismological Society of America, v. 66, No.4.

Hunter, J.A., S.E. Pullan, R A. Burns, R.L. Good, J.B. Harris, A. Pugin, A. Skvortsov, N.N. Goriainov. 1998. Downhole seismic logging for high-resolution reflection surveying in unconsolidated overburden. Geophysics, v. 63, No. 4, pp. 1122-1479

Hunter, J.A.; H.L. Crow, G.R. Brooks, M. Pyne, D. Motazedian, M. Lamontagne, A.J.-M. Pugin, S.E. Pullan, T. Cartwright, M. Douma, R.A. Burns, R.L. Good; K. Kaheshi-Banab, R. Caron, M. Kolaj, I. Folahan, L. Dixon, K. Dion, A. Duxbury, A. Landriault, V. Ter-Emmanuil, A. Jones, G. Plastow, D. Muir. 2010. Seismic site classification and site period mapping in the Ottawa area using geophysical methods. Geological Survey of Canada, Open File 6273, 80 pages.

Hunter, J.A., and H.L. Crow, eds, 2012. Shear Wave Velocity Measurement Guidelines for Canadian Seismic Site Characterization in Soil and Rock. Geological Survey of Canada, Open File 7078, 227 p.

Molnar S., J.F. Cassidy, S. Castellaro, C. Cornou, H. Crow, J.A. Hunter, S. Matsushima, F.J. Sánchez-Sesma, A. Yong. 2018. Application of Microtremor Horizontal-to-Vertical Spectral Ratio (MHVSR) Analysis for Site Characterization: State of the Art. Surveys in Geophysics. doi.org/10.1007/s10712-018-9464-4.

Motazedian, D., K. Khaheshi-Banab, J.A. Hunter, S. Sivathayalan, H.L. Crow, G. Brooks. 2011, Comparison of Site Period Derived from Different Evaluation Methods. Bulletin of the Seismological Society of America, v. 101, No.6, p.2942-2954.

Motazedian , D., H. Torabi, J.A. Hunter, H.L. Crow, M. Pyne. 2020. Seismic Site Period Studies for Nonlinear Soil in the City of Ottawa, Canada. Journal of Soil Dynamics and Earthquake Engineering (in press).

Pullan, S.E., J.A. Hunter, and R.L. Good, 2002. Using Down-hole Geophysical Logs To Provide Detailed Lithological and Stratigraphic Assignment, Oak Ridges Moraine, Southern Ontario. Geological Survey of Canada, Current Research 2002-E8, 12p.

Rosset, P., L.E. Chouinard, 2009. Characterization of site effects in Montreal, Canada. Nat Hazards 48, 295–308. doi.org/10.1007/s11069-008-9263-1

SESAME 2004. Guidelines for the implementation of the H/V spectral ratio technique on ambient vibrations-Measurements, processing and interpretation. SESAME European research project, Deliverable D23. 12., Project No. EVG1-CT-2000-00026 SESAME, 62 pp.